REVIEW ARTICLE

Clinically Relevant Imaging in Tuberous Sclerosis

Rupa Radhakrishnan, Sadhna Verma

Department of Radiology, University of Cincinnati Medical Center, Cincinnati, OH, USA

Address for correspondence:
Dr. Sadhna Verma,
University of Cincinnati Medical Center, Department of Radiology,
234 Goodman Street,
PO Box 670761, Cincinnati,
OH 45267-0761, USA
E-mail: drsadhnaverma@gmail.com

ABSTRACT

Tuberous sclerosis (TS), also known as Bourneville disease or Bourneville–Pringle disease, is an autosomal dominant genetic disorder classically characterized by the presence of hamartomatous growths in multiple organs. TS and tuberous sclerosis complex (TSC) are different terms for the same genetic condition. Both terms describe clinical changes due to mutations involving either of the two genes named TSC1 and TSC2, which regulate cell growth. The diagnosis of TSC is established using diagnostic criteria based on clinical and imaging findings. Routine screening and surveillance of patients with TSC is needed to determine the presence and extent of organ involvement, especially the brain, kidneys, and lungs, and identify the development of associated complications. As the treatment is organ specific, imaging plays a crucial role in the management of patients with TSC.

Key words: Angiomyolipomas, lymphangioleiomyomatosis, tubers

INTRODUCTION

Tuberous sclerosis complex (TSC) is a rare autosomal dominant neurocutaneous syndrome characterized by the presence of benign congenital tumors in multiple organs. It has a birth incidence of 1:6000, with over two-thirds of cases being sporadic from new mutations. TSC can affect virtually any organ system[1-3] and all racial groups. Hamartomas in TSC patients are frequently present in the skin, brain, kidneys, and heart. Less frequently, hamartomas involve the lungs, retina, gingiva, bones, and gastrointestinal tract.[4]

TSC most often presents with neurologic symptoms, with approximately 90% of affected individuals experiencing seizures and about half the patients experiencing cognitive impairment, autism, or other behavioral disorders. Neurologic symptoms are generally due to hamartomas. Renal manifestations are the second most common finding associated with TSC, with angiomyolipomas (AMLs) occurring in 80%, and renal cystic disease in 50% of the patients. Pulmonary involvement, specifically lymphangioleiomyomatosis (LAM), is the third most common cause of TSC associated morbidity, occurring in approximately 35% of female TSC patients.

The classic Vogt's triad (facial angiofibromas, mental retardation, and intractable epilepsy) is present in less than 40% of affected patients. In a consensus conference in 1998,

Access this article online	
Quick Response Code:	**Website:** www.clinicalimagingscience.org
	DOI: 10.4103/2156-7514.83230

Roach et al[5] revised the clinical diagnostic criteria of TSC to provide a standardized approach for identification of this disease. There are many features that are commonly present in TSC, but not necessarily diagnostic in isolation, as they may also be seen in a small percentage of the normal population, thus necessitating a standardized approach. Features that were more specific for TSC formed the major features and features that were less specific for TSC were included in the minor features. Both objective clinical signs and imaging findings were included. Some features that were occasionally seen together in the unaffected population (such as cortical tubers and white matter migration lines) were considered a single criterion if present together in TSC [Table 1]. The presence of typical imaging features of TSC may help to confirm diagnosis in patients with suspected TSC.

GENETIC BASIS

TSC is caused by mutations in either of the two tumor suppressor genes known as *TSC1* and *TSC2* that have been mapped by linkage analysis in multigenerational families and positional cloning.[6,7] The *TSC1* gene consists of 23 exons located on the long arm of chromosome 9 (9q34) and encodes a 130-kDa protein called hamartin. The *TSC2* gene consists of 41 exons on the short arm of chromosome 16 (16p13) and encodes a 200-kDa protein called tuberin. The location of the *TSC2* gene is contiguous with the *PKD1* gene, which is involved in polycystic kidney disease, and this proximity may explain the presence of multiple renal cysts in patients with TSC.[8] More than 200 *TSC1* and almost 700 *TSC2* allelic variants have been reported.[9,10] Pathogenic mutations can be identified in up to 85% of TSC patients using current genetic tests.[11]

Hamartin and tuberin interact with high affinity to form a complex in multiple organs, such as the kidneys, brain, lungs, and pancreas. In these organs, the hamartin–tuberin complex plays a critical role in the integration of cellular sensory input including cellular energy supply, growth factors, genomic integrity, and growth substrate availability. Advances in cytogenetics and pathophysiology have brought to light the functions of the hamartin–tuberin heterodimer. Normally, tuberin is inactivated by direct phosphorylation, resulting in downregulation of the *Ras* homologue expressed in brain (*Rheb*), a specific GTPase that in turn blocks the activity of the main mammalian regulator of cell growth and proliferation, mTOR kinase. Hamartin is also believed to influence mTOR activation.[1] If either tuberin or hamartin is absent, as in TSC, mTOR is upregulated, enabling cell growth and proliferation.[12] Loss of heterozygosity of the *TSC1* or *TSC2* gene is identified in most renal AMLs, subependymal giant cell astrocytomas (SEGAs) in the brain and cardiac rhabdomyomas.[13,14]

CNS LESIONS

The common brain lesions encountered in TSC include cortical and subcortical tubers, subependymal nodules (SENs), SEGAs, and white matter lesions.[15,16] Estimated prevalence of cortical tuber and/or SENs is 95–100% and that of white matter abnormalities is 40–90%.[17-20] Cortical tubers and SENs have been diagnosed *in utero* with fetal magnetic resonance imaging (MRI) as early as the second trimester.[21] In addition to the classic intracranial lesions in TSC, developmental dysplasias of the brain are described that are less commonly identified. Cortical dysplasia may range from focal gyriform abnormalities and heterotopias to more extensive lobar migration abnormalities such as schizencephaly. Large segments of cortical dysplasia involving entire lobes or a hemisphere, termed transmantle cortical dysplasia, may be present, with characteristic calcifications when associated with TSC.[22] Partial agenesis of the corpus callosum has been described in TSC. There are several case reports of intracranial aneurysms, frequently in the anterior circulation. Intracranial moyamoya vasculopathy has also been described as a consequence of carotid artery disease in a few patients. Ventricular enlargement may be seen secondary to hydrocephalus or due to volume loss in dysplastic brain.[23,24] Infratentorial lesions are less commonly identified in patients with TSC. Apart from tubers, SENs and white matter lesions, less frequent infratentorial lesions include cerebellar dysplasia, cerebellar folia or white matter calcifications, cerebellar hyperplasia, and chiari malformation.[23,24]

Cortical tubers

Cortical tubers are areas of markedly disorganized cortex with loss of the normal six-layer architecture of the cortex. These regions contain aggregates of abnormal glial and dysplastic neuronal elements including giant cells or balloon cells, which are characteristic of tubers. Cortical tubers are mostly supratentorial, in the frontal lobes, although

Table 1: Clinical diagnostic criteria for TSC	
Major features	**Minor features**
Facial angiofibromas	"Confetti" skin lesions
Hypomelanotic macules	Gingival fibromas
Shagreen patches	Pits in dental enamel
Cortical tubers	Cerebral white matter radial migration lines
Subependymal nodules	Retinal achromatic patches
Subependymal giant cell tumors	Bone cysts
Retinal hamartomas	Hamartomatous rectal polyps
Cardiac rhabdomyomas	
Renal AML	
Pulmonary LAM	

Definite diagnosis : two major features or one major and two minor features, Probable diagnosis: one major feature and one minor feature, Possible diagnosis: one major feature or two or more minor features, Note — Cortical tubers together with cerebral white matter radial migration lines are counted as one feature. In patients with LAM or renal AML, other features are required for diagnosis.[5]

infratentorial cerebellar tubers have been described as well.[25] The number and location of these tubers is associated with the degree of cerebral dysfunction including cognitive impairment, seizures, and autism.[26-28] There have been attempts to describe clinical severity based on MRI imaging characteristics [T1, T2, and fluid attenuated inversion recovery (FLAIR) signal] of cortical tubers,[29] but larger studies are needed to establish reliable criteria.

MRI is the most sensitive modality in the identification of cortical tubers that are commonly located at the gray–white junction, but frequently involve the overlying cortex and the subcortical white matter. Often, the cortex overlying a tuber is dysplastic and may demonstrate pachygyria or polymicrogyria. In older children and adults, the tubers have low signal on T1-weighted images and are hyperintense on T2-weighted and FLAIR images. In neonates and infants, with a background of unmyelinated white matter, cortical tubers have high signal on T1-weighted images and low signal on T2-weighted images. Due to variable T2 white matter signal in neonates, cortical tubers can be difficult to detect on T2-weighted imaging. Tubers frequently demonstrate central cavitation or calcification (50%), and approximately 10% of tubers demonstrate enhancement following contrast administration [Figure 1].

Occasionally, cortical tubers act as epileptogenic foci and may be treated with surgical resection if antiepileptic medication is ineffective. MRI, electroencephalography (EEG), and nuclear medicine imaging techniques such as positron emission tomography (PET) and single-photon emission computed tomography (SPECT) are used to localize the epileptogenic focus before surgery [Figure 2]. Ictal SPECT imaging can demonstrate increased radiotracer activity corresponding to increased perfusion in the epileptogenic region.
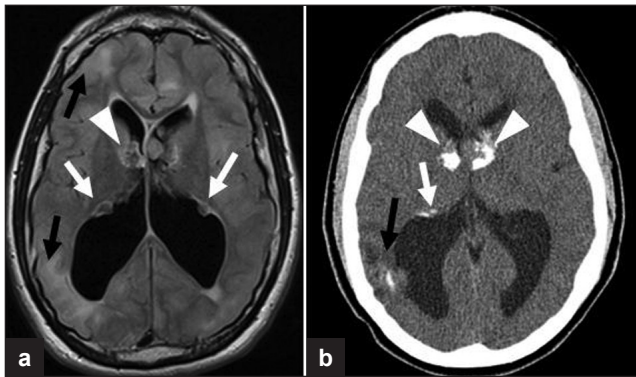

Figure 1: A 21-year-old woman with tuberous sclerosis. (a) Axial T2-weighted images of the brain at multiple levels. There is a dominant hyperintense T2 lesion in the left temporal cortex and subcortical region consistent with cortical tuber (white arrows). (b) Cortical tubers are also seen in the right insula and right parieto-occipital region (white arrows). There is a prominent subependymal nodule at the foramen of Monro (arrowhead). (c) Smaller subependymal nodules are identified along the walls of the lateral ventricle (black arrows).
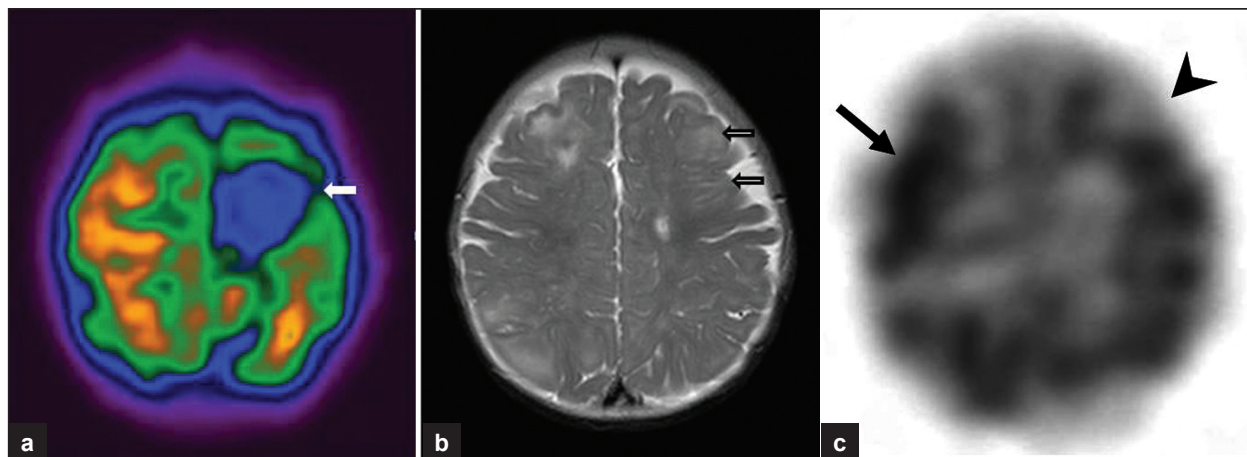
Figure 2: A 9-month-old boy with tuberous sclerosis. (a) Color-coded axial PET image through the brain shows a focus of decreased radiotracer activity in the left frontal convexity. (b) Axial T2-weighted MRI through a comparable location demonstrates multiple hyperintense cortical and subcortical lesions, one of which corresponds to the hypometabolic focus on PET. (c) Axial ictal brain perfusion scan shows persistent decreased activity in the region of tuber in the left cerebral cortex (arrowhead), with increased radiotracer activity in the right frontal region indicating an epileptogenic focus (arrow).
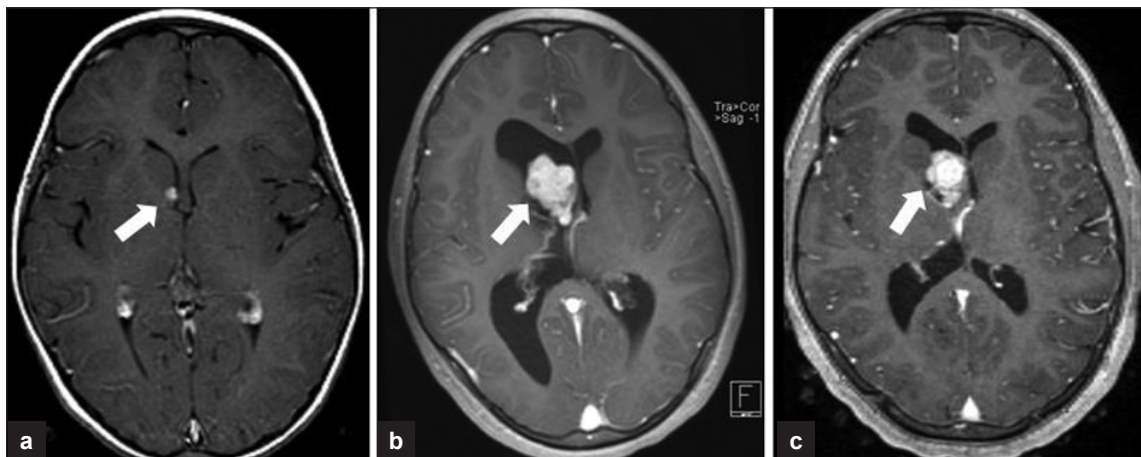
Subependymal nodules

SENs are present in about 80% of TS patients and are located around the wall of the lateral and third ventricle, usually in close proximity to the foramen of Monro.[25] Histologically, SENs contain large cells, similar to giant cells seen in tubers and elongated glial cells and are covered by a thin layer of ependyma. On MR imaging, these lesions are isointense or hyperintense on T2-weighted sequences and hyperintense on T1-weighted sequences. SENs may also demonstrate central low T2 signal with surrounding hyperintense T2 rim.[19] Variable enhancement may be demonstrated following contrast administration. SENs are more prone to calcification than cortical tubers, particularly at an early age, and are readily detected by computed tomography (CT) or susceptibility weighted imaging [Figure 3]. SENs typically measure less than 1 cm in size, but may grow over time and give rise to SEGAs.

Figure 3: A 20-year-old woman with tuberous sclerosis. (a) Axial FLAIR MR shows small subependymal nodules along the lateral walls of the lateral ventricles (white arrows) and heterogeneous masses at the foramen of Monro that likely represent subependymal giant cell astrocytomas (arrowheads). There is cortical and sub-cortical bright signal indicating tubers (black arrows). (b) Noncontrast head CT at the corresponding location shows calcifications at the subependymal giant cell astrocytomas (arrowheads), subependymal nodules (white arrows) and cortical tuber (black arrows) on the right.

Subependymal giant cell astrocytomas

SEGAs, although rare, are the most common brain tumors, occurring in up to 26% of TSC patients. The peak age of SEGA is during adolescence, although they have also been identified *in utero*. Microscopically, SEGAs consist of a mixed cell population of dysmorphic glial cells and giant cells with a rich vascular stroma. They are WHO grade 1 tumors with slow growth, minimal parenchymal invasion, absence of adjacent brain edema and no predilection for CSF spread. It is widely accepted that SEGAs arise from SENs, and serial CTs demonstrating growth of SEN into SEGA have been described [Figure 4].[30] Intermediate cells are identified between hamartomatous SEN and SEGA.[30] SEGAs commonly are located at the foramen of Monro, and their rapid growth can result in rather acute obstructive hydrocephalus. SENs near foramen of Monro, that increase in size over time, should be viewed as suspicious for SEGA. SEGAs are heterogeneous on MR imaging (T1 iso/hypointense, T2/FLAIR iso/hyperintense), contain calcifications, and demonstrate intense inhomogeneous enhancement. With the development of non-communicating hydrocephalus, transependymal flow of CSF may be apparent. In view of their vascular nature, CT and MRI may be useful in noninvasive assessment prior to surgery and in yearly screening during the high-risk period (8–18 years). MR spectroscopy may be useful in distinguishing SEGAs with high Cho/Cr and low NAA/Cr ratios from SENs.[31] In the absence of stigmata of TSC, a mass at the foramen of Monro may bring forth a differential diagnosis of choroid plexus papilloma, meningioma or neurocytoma. Choroid plexus papillomas are more common in infants than in adults, where they typically are located in the atrium of the lateral ventricle. Neurocytomas are usually attached to the septum pellucidum, and meningiomas, although


Figure 4: Sequential gadolinium-enhanced, axial T1-weighted images through the brain. (a) At 12 years of age, the image demonstrates a small, enhancing subdpendymal nodule near the foramen of Monro on the right. (b) At 20 years of age, there is a large, enhancing lobulated lesion in this location which developed in a span of 8 years, consistent with a subependymal giant cell astrocytoma. (c) At 21 years, there is mild decrease in the size of subependymal giant cell astrocytoma following initiation of rapamycin.

rare in this location, are typically attached to the choroid plexus when intraventricular.

SEGAs are usually followed by MRI for changes in size and onset of hydrocephalus, which may necessitate CSF diversion procedures, such as placement of a ventriculoperitoneal shunt. Surgical resection of SEGA is curative with good outcome and a low recurrence rate. Currently, surgery is planned before the onset of obstructive hydrocephalus. Sirolimus and everolimus are therapeutic agents, and both act by inhibiting mTOR (see above); they are used for management of SEGA in nonsurgical candidates. Everolimus has recently been approved by the FDA (in 2010) for treating SEGA.

White matter lesions

Superficial white matter abnormalities, radial white matter bands, and white matter cystic lesions occur in TSC. While white matter abnormalities can occur in all parts of the brain, they are most frequent in the frontal and parietal lobes and occasionally occur in the cerebellum.[19] Superficial white matter abnormalities are associated with almost all cortical tubers and exhibit T2 hyperintensity reflecting gliosis or decreased myelin content. Radial white matter bands are radiating lines of abnormal bright T2 and FLAIR signal extending from the periventricular regions into the subcortical white matter and are believed to represent lines of arrested neuronal migration. In the incompletely myelinated brain, white matter lesions are hyperintense to unmyelinated white matter on T1-weighted sequences and iso to hypointense to the white matter on T2-weighted sequences[19] [Figure 5]. Cysts are present in approximately 44% of patients with TSC and are frequently smaller than 1 cm and located adjacent to the occipital horn or trigone of the lateral ventricle. These cysts follow CSF signal on all sequences and may be septated or demonstrate peripheral enhancement. The etiology of these cysts is unclear.[18]
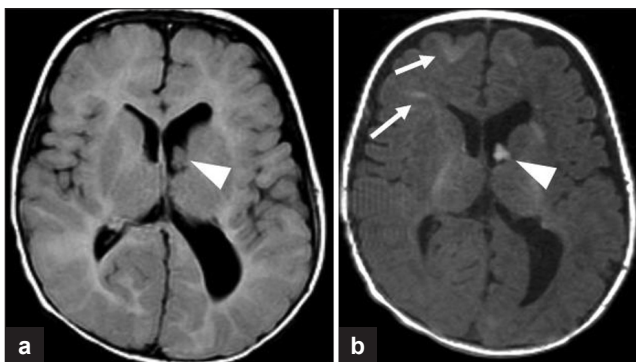
Figure 5: A 4-month-old infant with growth retardation. (a) Axial FLAIR image demonstrates a subependymal nodule at the foramen of Monro (arrowheads), but no definite white matter changes. (b) Corresponding T1-weighted image better demonstrates the white matter and cortical lesions (arrows) in this infant with incomplete myelination

RENAL INVOLVEMENT

Renal manifestations are the second most common findings associated with TSC. Both renal cystic disease and AMLs cause chronic renal disease, affecting approximately 1 million patients with TSC worldwide. Using death certificate data, Shepherd et al identified renal failure as the leading cause of death in adult patients with TSC at the Mayo Clinic.[32]

Renal angiomyolipomas

Benign AMLs are the most common renal lesions in adults and older children with TSC.[1,33] In comparison to sporadic AMLs, renal AMLs in TSC develop in early childhood, grow throughout adolescence and stabilize by adulthood.[34,35] While approximately 80% of adolescents and adults with TSC have AMLs, only approximately 20% of patients with AML have TS.[36]

AMLs are the most common tumor occurring in the kidney and are typically benign. They contain variable amounts of vasculature, immature smooth muscle cells, epithelioid cells, and fat cells, all of which are deficient in either tuberin or hamartin. This deficiency may disrupt the integrated control of cell growth, leading to the AMLs.[37] Renal AMLs exhibit immunoreactivity for both melanocytic markers and smooth muscle markers.[38]

The typical appearance of an AML on CT is a noncalcified cortical mass containing fat attenuation of less than −20 HU[36] [Figure 6]. In addition to macroscopic disease, renal tissue that is radiologically normal may contain microscopic AMLs.[38] It is unclear if these microscopic lesions may grow with age.

Lipid-poor lesions in patients with TSC account for 4.5–33% of AMLs.[39,40] Lipid-poor lesions are defined as having less

Figure 6: A 45-year-old woman with tuberous sclerosis. Axial noncontrast CT image through the abdomen demonstrates enlarged kidneys with fat attenuation lesions in both kidneys consistent with angiomyolipomas

than 25% fat per high-power field,[41] on average contain 4.1% fat.[42] Lipid-poor TSC associated AML may consist of predominantly spindle cells, epithelioid cells, or vascular elements.[38] Lipid-poor AMLs are clinically relevant due to their differing clinical course and difficult distinction from renal cell carcinoma. Radiographic features that may help differentiate AML from renal cell cancer (RCC) are homogenous enhancement on CT, lack of calcifications and homogenous isoechogenicity on ultrasound.[39,43] At present, there is no standard CT Hounsfield value to separate lipid poor-AML from RCC.[44-46] Use of AMLs' growth rate has been presented as a possible method to distinguish more ominous lesions such as RCC from lipid-poor AML.[47] Utilization of MR imaging artifacts such as in-phase/out-of-phase techniques and chemical shift artifact can assist in identifying fat in lipid-poor lesions.[48,49] If concern remains, PET scans can be helpful because AMLs are generally not PET avid.[50,51] If there is concern for RCC and tissue diagnosis is essential, biopsy may be considered. Epithelioid AML can exhibit an aggressive phenotype, with metastasis and recurrence,[52] local invasion, including extension into renal vein or inferior vena cava,[53] and lymph node involvement.[54,55] Distinction of these aggressive AMLs from renal cancer is difficult by imaging and these lesions are generally managed surgically.

The blood vessels within AMLs are abnormal with no internal elastic lamina. The smooth muscle is replaced by fibrous tissue and these vessels are rigid, tortuous, and prone to aneurysm formation and rupture,[56] making them clinically important. The hemorrhage risk of renal AML in TSC patients is between 25% and 50%.[57,58]

Approximately 60% of patients with AML will be symptomatic at diagnosis, most commonly presenting with a combination of acute bleeding, flank pain, hematuria, or tender mass.[59] The risk of hemorrhage is associated with the size of the AML (greater than 4 cm) and size of the aneurysm (greater than 5 mm), the latter having higher sensitivity and specificity.[60] Control of active bleeding and prevention of re-bleeding are achieved by embolization of the aneurysm,[61,62] that preserves most of the renal parenchyma[63] [Figure 7]. On angiogram in the acute setting, localizing the symptomatic aneurysm can be difficult, as active extravasation is rare and there is typically extensive abnormal vasculature. The "light bulb sign", identified in 70% of patients treated following an acute bleed, may help in localization of the bleeding aneurysm. The light bulb sign is caused by a perianeurysmal hematoma displacing the surrounding tissue and vessels, causing a "filling defect" seen on all phases of the angiogram.[64] Corticosteroid therapy decreases subsequent postembolization syndrome.[61]

Surgical therapy is employed for a specifically targeted lesion, such as an exophytic nonbleeding AMLs, with minimal risk to the remainder of the kidney. Less invasive surgical methods such as laparoscopy, partial nephrectomy or ablative therapy with cryotherapy or radiofrequency treatment have reduced the overall impact of surgery.

Renal cystic disease

Renal cysts, usually multiple and bilateral, are the second most common kidney lesion, occurring in approximately 18–53% of patients with TSC.[8,65,66] Although renal cysts may occasionally be present in the fetus and neonate, typically children with TSC are born with normal kidneys and develop cystic disease and AML as they age.[32,34] Two percent of patients with TSC have severe early onset of polycystic phenotype associated with deletions involving adjacent *TSC2* and *PKD1* genes on chromosome 16p13.3.[8]

Renal cystic disease may be macrocystic, or microcystic and undetectable by imaging studies. Inactivation of the tuberin–hamartin complex is thought to result in ciliary dysfunction and defects in cell polarity leading to cyst formation.[67] In patients with TSC, cysts may arise from all segments of the nephron, including the renal tubules

Figure 7: (a–c) A 39-year-old woman with tuberous sclerosis. Axial contrast-enhanced CT images though the abdomen show multiple bilateral fat density lesions consistent with renal angiomyolipomas. Angiogram image demonstrates coiling of an aneurysm within an angiomyolipoma in the left kidney. The contrast-enhanced CT image on the right demonstrate volume loss in the left kidney following embolization

and the glomeruli.[68,69] Animal models demonstrate acute acceleration of renal cystic disease following acute renal injury, which may also be the case in humans[70] [Figure 8a].

Renal cell cancer

The overall incidence of RCC in TSC patients is similar to that in the general population, with a lifetime risk of 2–3%.[1,71] RCC manifests at an earlier age in patients with TS (mean age 28 years) than in the general population (mean age 53 years) and shows greater histological variety with clear cell, papillary and chromophobe subtypes.[1,24] Growth of RCC in TSC patients is slower than sporadic RCC.[72]

CARDIAC LESIONS

In patients with TSC, cardiac rhabdomyoma [Figure 9] is the most commonly identified *in utero*, infancy, and early childhood. Childhood tumor regression is the rule, with most of them regressing before birth and 70% by the age of 4 years.[73] There may be a second peak in the incidence of these tumors in pubertal females with TSC.[74,75] Hormonal influence of progesterone has been suggested as a cause for the bimodal distribution.

These tumors are usually asymptomatic, but in a minority of cases may present with cardiac failure or arrhythmia when surgical resection may be considered. Echocardiography is commonly used in screening and follow-up of cardiac rhabdomyoma. MR imaging may provide additional information in complex cases.

PULMONARY LESIONS

The three main pulmonary lesions found in TSC are LAM, multifocal micronodular pneumocyte hyperplasia (MMPH), and clear cell "sugar" tumor (CCST) of the lung.

Lymphangioleiomyomatosis

LAM is the most common pulmonary lesion occurring essentially in only women, with the average age of onset being 33 years.[76] Pulmonary LAM is characterized by diffuse interstitial proliferation of bundles of smooth muscle cells and cystic change in pulmonary parenchyma. Dyspnea and recurrent spontaneous pneumothorax are the most common presentations, with slow and steady progression to respiratory failure.

On CT, the characteristic feature of LAM is thin-walled cysts of variable size and contour [Figure 10], which may communicate with the airways, indicated by decrease in size on expiratory imaging. In a patient with TSC, biopsy may be obviated by the presence of these characteristic findings. Occasionally, reticular opacities are identified that may represent interstitial edema due to lymphatic
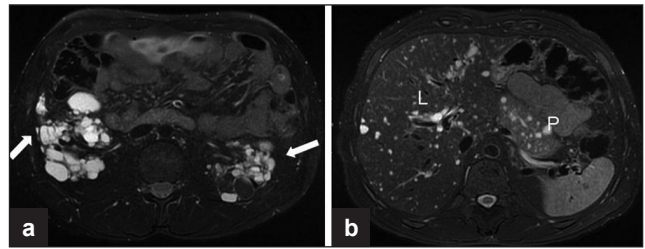
Figure 8: A 33-year-old woman with tuberous sclerosis. (a) Axial T2-weighted, fat-suppressed MR image through the kidneys shows bilateral hyperintense T2 renal cysts. Also note the hypointense lesions in the left kidney in the fat-suppressed sequence, consistent with angiomyolipomas. (b) Axial T2-weighted, fat-suppressed MR image through the upper abdomen shows numerous hyperintense T2 cysts in the liver (L) and pancreas (P)
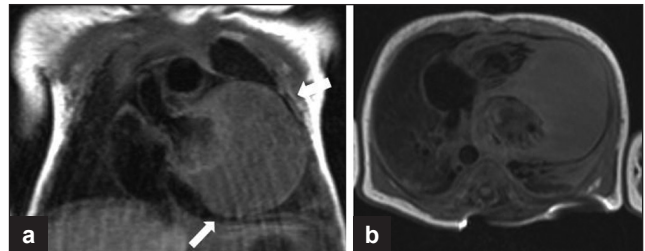
Figure 9: A 2-day-old infant with arrhythmia. Cardiac gated sagittal and axial T1-weighted images show a large homogeneous isointense lesion involving the cardiac apex and the apical portions of the septum and lateral wall consistent with cardiac rhabdomyoma. This child was later diagnosed with tuberous sclerosis
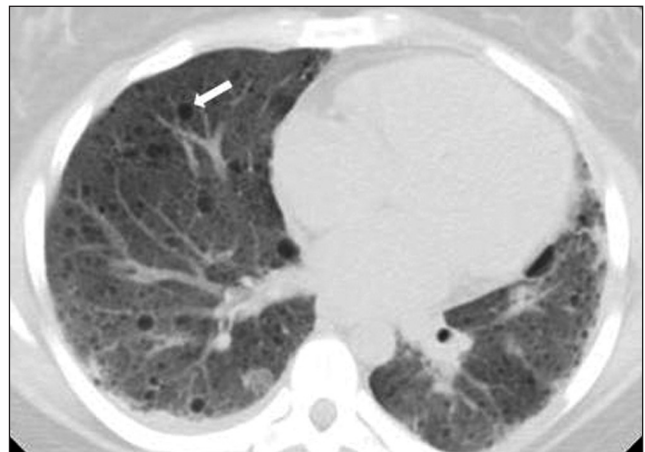
Figure 10: A 24-year-old woman with tuberous sclerosis. Axial noncontrast CT image through the chest demonstrates multiple small, thin-walled, round cysts (arrow) consistent with lymphangioleiomyomatosis

obstruction. Chylothorax and recurrent pneumothorax are complications which may be identified on imaging.

In the past decade, there have been several clinical trials on hormonal therapy with progesterone and estrogen in patients with LAM, identifying downregulation of progesterone receptors.[77,78] Progesterone is the most commonly used drug with a small case series and meta-analysis suggesting it to be helpful in one-third to one-half of the cases.[79,80] In nonresponders, surgical intervention, such as thoracic drainage, pleurectomy or pleurodesis, may be

necessary for chylothorax and recurrent pneumothorax. A combined heart and lung transplantation may be indicated for refractory LAM. Prior pleurodesis may complicate future lung transplantation.

Multifocal micronodular pneumocyte hyperplasia

MMPH is a rare disorder associated with TSC. MMPH presents as multicentric, well-demarcated hamartomatous nodules with proliferation of type II pneumocytes along the alveolar septa. MMPH also occurs predominantly in female patients and may occur with or without LAM.

On thin-section CT, MMPH is identified as multiple tiny, diffusely scattered nodules in a random distribution [Figure 11]. The appearance is nonspecific and difficult to distinguish from causes of multiple small nodules; however, in a patient with TSC, MMPH is considered with this pattern.[81] Isolated MMPH may present as dyspnea, cough, and mild to moderate hypoxemia,[82] but in view of its hamartomatous nature, it is not typically progressive or fatal.

Clear cell "sugar" tumors of the lung

CCSTs are rare benign lung lesions in TSC. These are typically unencapsulated and composed of round, oval, or focally spindled cells with distinct cellular borders, abundant clear to eosinophilic granular cytoplasm, prominent thin-walled blood channels, and focal hyaline stroma. Mitotic figures and necrosis are not usually seen.[83]

On imaging, CCSTs of the lung present as a rounded, smoothly marginated, peripheral parenchymal nodule or mass without evidence of cavitation or calcification. These lesions appear to avidly enhance on contrast-enhanced CT scans, likely related to rich vascular stroma.[84,85] While CCSTs are usually benign, certain aggressive cases have been documented, occurring almost exclusively in the lung.[86,87]

OTHER ABDOMINAL MANIFESTATIONS

Hepatic AMLs occur in about 13% of patients with TSC and are more common in females. Multiple hepatic AMLs may be
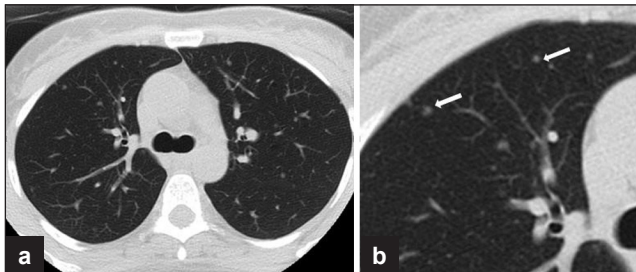
present in patients with bilateral diffuse renal AMLs. These lesions are similar histologically to the renal AMLs.[88] On CT evaluation, hepatic AMLs are round, well-circumscribed lesions containing areas of low attenuation consistent with fat. On ultrasound, they typically present as echogenic foci. No definite follow-up has been recommended for these lesions as they are benign. Occasionally, hepatic AMLs have been reported to rupture if larger than 4 cm.[88]

Splenic hamartomas are rarely identified in patients with TSC.[89] Multiple pancreatic lesions are described, including AML.[90] Biopsy is usually recommended for pancreatic lesions.

Hamartomatous colorectal polyps are a common finding in TSC. These are usually small, less than 5 mm in diameter, and sessile or occasionally filiform in appearance.[91,92]

LAM, although most common in the lungs, may also occur in other areas such as the retroperitoneum resulting in cystic lesions in the retroperitoneum and chylous ascites. Multicystic retroperitoneal lesions in a patient with TSC are considered to represent LAM. Retroperitoneal LAM can present with abdominal bloating and may cause lymphatic obstruction with lower extremity edema.
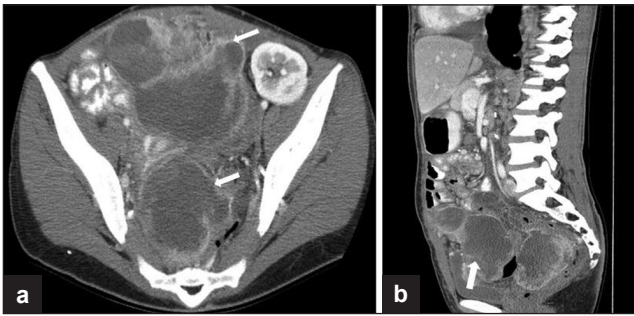
PEComas are a family of mesenchymal tumors consisting of perivascular epithelioid cells. The cell type from which these tumors originate remains unknown and has no normal counterpart. Genetically, PEComas are linked to the tuberous sclerosis genes *TSC1* and *TSC2*. PEComas bear significant histologic and immunohistochemical similarity to AML, LAM and CCST of the lung, and CCSTs in other organs, which some authors classify under the broad category of PEComas.[93] These tumors are of perivascular epithelioid origin with a clear/granular cytoplasm and central round nucleus without prominent nucleoli. PEComas typically stain for melanocytic markers and myogenic markers and have a variable radiologic appearance. These tumors and have been reported in the falciform ligament/ligamentum teres, uterus, abdominal cavity and mesentery, soft tissue, bone, and skin [Figure 12].

SKELETAL LESIONS

Multiple bony changes have been described in TSC of which sclerotic lesions are the most common[24] [Figure 13]. Hyperostosis of inner table of skull, periosteal new bone formation, scoliosis, and bone cysts[5] have also been described.

CONCLUSION

TSC is a multisystem disorder characterized by a wide

Figure 11: (a, b) A 38-year-old woman with tuberous sclerosis. Axial noncontrast CT image through the chest and an enlarged view (right) demonstrating small randomly distributed soft tissue nodules, consistent with multifocal micronodular pneumocyte hyperplasia

Figure 12: A 35-year-old female with tuberous sclerosis and lymphangioleiomyomatosis. Status post-renal transplant. (a) Axial and (b) sagittal contrast-enhanced CT images show large, irregular, low-attenuation enhancing, peripherally enhancing masses in the pelvis in a patient with tuberous sclerosis, biopsy proven as PEComa (perivascular epitheliod cell tumor). Also note the transplant kidney in the left pelvis
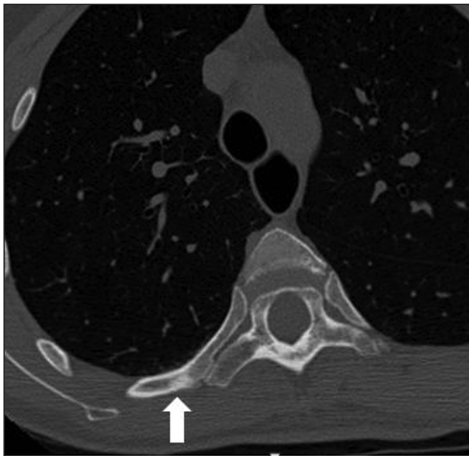
Figure 13: A 30-year-old with tuberous sclerosis. Axial noncontrast chest CT demonstrates multiple small sclerotic lesions in the ribs and vertebrae

spectrum of clinical and imaging features. Due to better testing and imaging methods, estimates of TSC frequency have risen dramatically in the recent years as individuals with less severe manifestations of the disorder are identified. Recognition of specific radiologic features may aid in early diagnosis and management and improve outcomes in TSC patients. Identification of patients at risk for severe manifestations of TSC and understanding the clinical impact of different radiological findings in TSC patients is crucial to improve management and outcomes.

REFERENCES

1. Crino PB, Nathanson KL, Henske EP. The tuberous sclerosis complex. N Engl J Med 2006;355:1345-56.
2. Yates JR. Tuberous sclerosis. Eur J Hum Genet 2006;14:1065-73.
3. Ruggieri M, Carbonara C, Magro G, Migone N, Grasso S, Tinè A, et al. Tuberous sclerosis complex: Neonatal deaths in three of four children of consanguineous, non-expressing parents. J Med Genet 1997;34:256-60.
4. Kwiatkowski DJ. Tuberous sclerosis: From tubers to mTOR. Ann Hum Genet 2003;67:87-96.
5. Roach ES, Gomez MR, Northrup H. Tuberous sclerosis complex consensus conference: Revised clinical diagnostic criteria. J Child Neurol 1998;13:624-8.
6. Kandt RS, Haines JL, Smith M, Northrup H, Gardner RJ, Short MP,

7. et al. Linkage of an important gene locus for tuberous sclerosis to a chromosome 16 marker for polycystic kidney disease. Nat Genet 1992;2:37-41.
7. van Slegtenhorst M, de Hoogt R, Hermans C, Nellist M, Janssen B, Verhoef S, et al. Identification of the tuberous sclerosis gene TSC1 on chromosome 9q34. Science 1997;277:805-8.
8. Sampson JR, Maheshwar MM, Aspinwall R, Thompson P, Cheadle JP, Ravine D, et al. Renal cystic disease in tuberous sclerosis: Role of the polycystic kidney disease 1 gene. Am J Hum Genet 1997;61:843-51.
9. Jones AC, Shyamsundar MM, Thomas MW, Maynard J, Idziaszczyk S, Tomkins S, et al. Comprehensive mutation analysis of TSC1 and TSC2- and phenotypic correlations in 150 families with tuberous sclerosis. Am J Hum Genet 1999;64:1305-15.
10. Sancak O, Nellist M, Goedbloed M, Elfferich P, Wouters C, Maat-Kievit A, et al. Mutational analysis of the TSC1 and TSC2 genes in a diagnostic setting: Genotype--phenotype correlations and comparison of diagnostic DNA techniques in Tuberous Sclerosis Complex. Eur J Hum Genet 2005;13:731-41.
11. Curatolo P, Bombardieri R, Jozwiak S. Tuberous sclerosis. Lancet 2008;372:657-68.
12. Kwiatkowski DJ, Manning BD. Tuberous sclerosis: A GAP at the crossroads of multiple signaling pathways. Hum Mol Genet 2005;14:R251-8.
13. Henske EP, Scheithauer BW, Short MP, Wollmann R, Nahmias J, Hornigold N, et al. Allelic loss is frequent in tuberous sclerosis kidney lesions but rare in brain lesions. Am J Hum Genet 1996;59:400-6.
14. Henske EP, Wessner LL, Golden J, Scheithauer BW, Vortmeyer AO, Zhuang Z, et al. Loss of tuberin in both subependymal giant cell astrocytomas and angiomyolipomas supports a two-hit model for the pathogenesis of tuberous sclerosis tumors. Am J Pathol 1997;151:1639-47.
15. Mizuguchi M, Takashima S. Neuropathology of tuberous sclerosis. Brain Dev 2001;23:508-15.
16. Vinters HV. Russel and Rubensten's Pathology of Tumors of the Nervous System. 7th ed. London: Hodder Arnold Publication; 2006.
17. O'Callaghan FJ, Martyn CN, Renowden S, Noakes M, Presdee D, Osborne JP. Subependymal nodules, giant cell astrocytomas and the tuberous sclerosis complex: A population-based study. Arch Dis Child 2008;93:751-4.
18. Van Tassel P, Cure JK, Holden KR. Cystlike white matter lesions in tuberous sclerosis. AJNR Am J Neuroradiol 1997;18:1367-73.
19. Braffman BH, Bilaniuk LT, Naidich TP, Altman NR, Post MJ, Quencer RM, et al. MR imaging of tuberous sclerosis: Pathogenesis of this phakomatosis, use of gadopentetate dimeglumine, and literature review. Radiology 1992;183:227-38.
20. Nixon JR, Houser OW, Gomez MR, Okazaki H. Cerebral tuberous sclerosis: MR imaging. Radiology 1989;170:869-73.
21. Levine D, Barnes P, Korf B, Edelman R. Tuberous sclerosis in the fetus: Second-trimester diagnosis of subependymal tubers with ultrafast MR imaging. AJR Am J Roentgenol 2000;175:1067-9.
22. Vigliano P, Canavese C, Bobba B, Genitori L, Papalia F, Padovan S, et al. Transmantle dysplasia in tuberous sclerosis: Clinical features and surgical outcome in four children. J Child Neurol 2002;17:752-8.
23. DiMario FJ Jr. Brain abnormalities in tuberous sclerosis complex. J Child Neurol 2004;19:650-7.
24. Umeoka S, Koyama T, Miki Y, Akai M, Tsutsui K, Togashi K. Pictorial review of tuberous sclerosis in various organs. Radiographics 2008;28:e32.
25. Grajkowska W, Kotulska K, Jurkiewicz E, Matyja E. Brain lesions in tuberous sclerosis complex. Review. Folia Neuropathol 2010;48:139-49.
26. Kassiri J, Snyder TJ, Bhargava R, Wheatley BM, Sinclair DB. Cortical tubers, cognition, and epilepsy in tuberous sclerosis. Pediatr Neurol 2011;44:328-32.
27. Goodman M, Lamm SH, Engel A, Shepherd CW, Houser OW, Gomez MR. Cortical tuber count: A biomarker indicating neurologic severity

of tuberous sclerosis complex. J Child Neurol 1997;12:85-90.

28. Curatolo P, Porfirio MC, Manzi B, Seri S. Autism in tuberous sclerosis. Eur J Paediatr Neurol 2004;8:327-32.

29. Gallagher A, Grant EP, Madan N, Jarrett DY, Lyczkowski DA, Thiele EA. MRI findings reveal three different types of tubers in patients with tuberous sclerosis complex. J Neurol 2010;257:1373-81.

30. Morimoto K, Mogami H. Sequential CT study of subependymal giant-cell astrocytoma associated with tuberous sclerosis. Case report. J Neurosurg 1986;65:874-7.

31. de Carvalho Neto A, Gasparetto EL, Bruck I. Subependymal giant cell astrocytoma with high choline/creatine ratio on proton MR spectroscopy. Arq Neuropsiquiatr 2006;64:877-80.

32. Shepherd CW, Gomez MR, Lie JT, Crowson CS. Causes of death in patients with tuberous sclerosis. Mayo Clin Proc 1991;66:792-6.

33. Ewalt DH, Sheffield E, Sparagana SP, Delgado MR, Roach ES. Renal lesion growth in children with tuberous sclerosis complex. J Urol 1998;160:141-5.

34. Gomez MR, Whittemore VH, editors. Tuberous sclerosis complex developmental perspectives in psychiatry. New York: Oxford University press; 1999.

35. O'Callaghan FJ, Harris T, Joinson C, Bolton P, Noakes M, Presdee D, et al. The relation of infantile spasms, tubers, and intelligence in tuberous sclerosis complex. Arch Dis Child 2004;89:530-3.

36. Logue LG, Acker RE, Sienko AE. Best cases from the AFIP: Angiomyolipomas in tuberous sclerosis. Radiographics 2003;23:241-6.

37. Siroky BJ, Yin H, Bissler JJ. Clinical and molecular insights into tuberous sclerosis complex renal disease. Pediatr Nephrol 2011;26:839-52.

38. Dixon BP, Hulbert JC, Bissler JJ. Tuberous sclerosis complex renal disease. Nephron Exp Nephrol 2011;118:e15-20.

39. Kim JK, Park SY, Shon JH, Cho KS. Angiomyolipoma with minimal fat: Differentiation from renal cell carcinoma at biphasic helical CT. Radiology 2004;230:677-84.

40. Pereira JM, Sirlin CB, Pinto PS, Casola G. CT and MR imaging of extrahepatic fatty masses of the abdomen and pelvis: Techniques, diagnosis, differential diagnosis, and pitfalls. Radiographics 2005;25:69-85.

41. Milner J, McNeil B, Alioto J, Proud K, Rubinas T, Picken M, et al. Fat poor renal angiomyolipoma: Patient, computerized tomography and histological findings. J Urol 2006;176:905-9.

42. Hafron J, Fogarty JD, Hoenig DM, Li M, Berkenblit R, Ghavamian R. Imaging characteristics of minimal fat renal angiomyolipoma with histologic correlations. Urology 2005;66:1155-9.

43. Jinzaki M, Tanimoto A, Narimatsu Y, Ohkuma K, Kurata T, Shinmoto H, et al. Angiomyolipoma: Imaging findings in lesions with minimal fat. Radiology 1997;205:497-502.

44. Simpson E, Patel U. Diagnosis of angiomyolipoma using computed tomography-region of interest < or =-10 HU or 4 adjacent pixels < or =-10 HU are recommended as the diagnostic thresholds. Clin Radiol 2006;61:410-6.

45. Kim JY, Kim JK, Kim N, Cho KS. CT histogram analysis: Differentiation of angiomyolipoma without visible fat from renal cell carcinoma at CT imaging. Radiology 2008;246:472-9.

46. Lane BR, Aydin H, Danforth TL, Zhou M, Remer EM, Novick AC, et al. Clinical correlates of renal angiomyolipoma subtypes in 209 patients: Classic, fat poor, tuberous sclerosis associated and epithelioid. J Urol 2008;180:836-43.

47. Patel U, Simpson E, Kingswood JC, Saggar-Malik AK. Tuberose sclerosis complex: Analysis of growth rates aids differentiation of renal cell carcinoma from atypical or minimal-fat-containing angiomyolipoma. Clin Radiol 2005;60:665-73; discussion 663-4.

48. Mitchell DG, Crovello M, Matteucci T, Petersen RO, Miettinen MM. Benign adrenocortical masses: Diagnosis with chemical shift MR imaging. Radiology 1992;185:345-51.

49. Israel GM, Hindman N, Hecht E, Krinsky G. The use of opposed-phase chemical shift MRI in the diagnosis of renal angiomyolipomas. AJR

Am J Roentgenol 2005;184:1868-72.

50. Young LR, Franz DN, Nagarkatte P, Fletcher CD, Wikenheiser-Brokamp KA, Galsky MD, et al. Utility of [18F]2-fluoro-2-deoxyglucose-PET in sporadic and tuberous sclerosis-associated lymphangioleiomyomatosis. Chest 2009;136:926-33.

51. Jiang X, Kenerson H, Aicher L, Miyaoka R, Eary J, Bissler J, et al. The tuberous sclerosis complex regulates trafficking of glucose transporters and glucose uptake. Am J Pathol 2008;172:1748-56.

52. Eble JN, Amin MB, Young RH. Epithelioid angiomyolipoma of the kidney: A report of five cases with a prominent and diagnostically confusing epithelioid smooth muscle component. Am J Surg Pathol 1997;21:1123-30.

53. Park HK, Zhang S, Wong MK, Kim HL. Clinical presentation of epithelioid angiomyolipoma. Int J Urol 2007;14:21-5.

54. Reiff DB, Dow J. Case report: Invasive renal angiomyolipoma--sonographic and CT features. Clin Radiol 1993;48:283-5.

55. Koo KC, Kim WT, Ham WS, Lee JS, Ju HJ, Choi YD. Trends of presentation and clinical outcome of treated renal angiomyolipoma. Yonsei Med J 2010;51:728-34.

56. Lendvay TS, Marshall FF. The tuberous sclerosis complex and its highly variable manifestations. J Urol 2003;169:1635-42.

57. Kessler OJ, Gillon G, Neuman M, Engelstein D, Winkler H, Baniel J. Management of renal angiomyolipoma: Analysis of 15 cases. Eur Urol 1998;33:572-5.

58. Mouded IM, Tolia BM, Bernie JE, Newman HR. Symptomatic renal angiomyolipoma: Report of 8 cases, 2 with spontaneous rupture. J Urol 1978;119:684-8.

59. Nelson CP, Sanda MG. Contemporary diagnosis and management of renal angiomyolipoma. J Urol 2002;168:1315-25.

60. Yamakado K, Tanaka N, Nakagawa T, Kobayashi S, Yanagawa M, Takeda K. Renal angiomyolipoma: Relationships between tumor size, aneurysm formation, and rupture. Radiology 2002;225:78-82.

61. Bissler JJ, Racadio J, Donnelly LF, Johnson ND. Reduction of postembolization syndrome after ablation of renal angiomyolipoma. Am J Kidney Dis 2002;39:966-71.

62. Williams JM, Racadio JM, Johnson ND, Donnelly LF, Bissler JJ. Embolization of renal angiomyolipomata in patients with tuberous sclerosis complex. Am J Kidney Dis 2006;47:95-102.

63. Ewalt DH, Diamond N, Rees C, Sparagana SP, Delgado M, Batchelor L, et al. Long-term outcome of transcatheter embolization of renal angiomyolipomas due to tuberous sclerosis complex. J Urol 2005;174:1764-6.

64. Lenton J, Kessel D, Watkinson AF. Embolization of renal angiomyolipoma: Immediate complications and long-term outcomes. Clin Radiol 2008;63:864-70.

65. Stillwell TJ, Gomez MR, Kelalis PP. Renal lesions in tuberous sclerosis. J Urol 1987;138:477-81.

66. Rakowski SK, Winterkorn EB, Paul E, Steele DJ, Halpern EF, Thiele EA. Renal manifestations of tuberous sclerosis complex: Incidence, prognosis, and predictive factors. Kidney Int 2006;70:1777-82.

67. Hartman TR, Liu D, Zilfou JT, Robb V, Morrison T, Watnick T, et al. The tuberous sclerosis proteins regulate formation of the primary cilium via a rapamycin-insensitive and polycystin 1-independent pathway. Hum Mol Genet 2009;18:151-63.

68. Saguem MH, Laarif M, Remadi S, Bozakoura C, Cox JN. Diffuse bilateral glomerulocystic disease of the kidneys and multiple cardiac rhabdomyomas in a newborn. Relationship with tuberous sclerosis and review of the literature. Pathol Res Pract 1992;188:367-73; discussion 373-4.

69. Bissler JJ, Siroky BJ, Yin H. Glomerulocystic kidney disease. Pediatr Nephrol 2010;25:2049-56; quiz 2056-9.

70. Patel V, Li L, Cobo-Stark P, Shao X, Somlo S, Lin F, et al. Acute kidney injury and aberrant planar cell polarity induce cyst formation in mice lacking renal cilia. Hum Mol Genet 2008;17:1578-90.

71. Pompili G, Zirpoli S, Sala C, Flor N, Alfano RM, Volpi A, et al. Magnetic resonance imaging of renal involvement in genetically studied patients with tuberous sclerosis complex. Eur J Radiol 2009;72:335-41.

72. Leung AK, Robson WL. Tuberous sclerosis complex: A review. J Pediatr Health Care 2007;21:108-14.

73. DiMario FJ Jr, Diana D, Leopold H, Chameides L. Evolution of cardiac rhabdomyoma in tuberous sclerosis complex. Clin Pediatr (Phila) 1996;35:615-9.

74. Jozwiak S, Kawalec W, Dluzewska J, Daszkowska J, Mirkowicz-Malek M, Michalowicz R. Cardiac tumours in tuberous sclerosis: Their incidence and course. Eur J Pediatr 1994;153:155-7.

75. Smith NM, Thornton CM. Fetal rhabdomyoma: Two instances of recurrence. Pediatr Pathol Lab Med 1996;16:673-80.

76. Castro M, Shepherd CW, Gomez MR, Lie JT, Ryu JH. Pulmonary tuberous sclerosis. Chest 1995;107:189-95.

77. Matsui K, Takeda K, Yu ZX, Valencia J, Travis WD, Moss J, et al. Downregulation of estrogen and progesterone receptors in the abnormal smooth muscle cells in pulmonary lymphangioleiomyomatosis following therapy. An immunohistochemical study. Am J Respir Crit Care Med 2000;161:1002-9.

78. Logginidou H, Ao X, Russo I, Henske EP. Frequent estrogen and progesterone receptor immunoreactivity in renal angiomyolipomas from women with pulmonary lymphangioleiomyomatosis. Chest 2000;117:25-30.

79. Kitaichi M, Nishimura K, Itoh H, Izumi T. Pulmonary lymphangioleiomyomatosis: A report of 46 patients including a clinicopathologic study of prognostic factors. Am J Respir Crit Care Med 1995;151:527-33.

80. Eliasson AH, Phillips YY, Tenholder MF. Treatment of lymphangioleiomyomatosis. A meta-analysis. Chest 1989;96:1352-5.

81. Ristagno RL, Biddinger PW, Pina EM, Meyer CA. Multifocal micronodular pneumocyte hyperplasia in tuberous sclerosis. AJR Am J Roentgenol 2005;184:S37-9.

82. Maruyama H, Seyama K, Sobajima J, Kitamura K, Sobajima T, Fukuda T, et al. Multifocal micronodular pneumocyte hyperplasia and lymphangioleiomyomatosis in tuberous sclerosis with a TSC2 gene. Mod Pathol 2001;14:609-14.

83. Flieder DB, Travis WD. Clear cell "sugar" tumor of the lung: Association with lymphangioleiomyomatosis and multifocal micronodular pneumocyte hyperplasia in a patient with tuberous sclerosis. Am J Surg Pathol 1997;21:1242-7.

84. Santana AN, Nunes FS, Ho N, Takagaki TY. A rare cause of hemoptysis: benign sugar (clear) cell tumor of the lung. Eur J Cardiothorac Surg 2004;25:652-4.

85. Ye T, Chen H, Hu H, Wang J, Shen L. Malignant clear cell sugar tumor of the lung: Patient case report. J Clin Oncol 2010;28:e626-8.

86. Sale GE, Kulander BG. 'Benign' clear-cell tumor (sugar tumor) of the lung with hepatic metastases ten years after resection of pulmonary primary tumor. Arch Pathol Lab Med 1988;112:1177-8.

87. Parfitt JR, Keith JL, Megyesi JF, Ang LC. Metastatic PEComa to the brain. Acta Neuropathol 2006;112:349-51.

88. Fricke BL, Donnelly LF, Casper KA, Bissler JJ. Frequency and imaging appearance of hepatic angiomyolipomas in pediatric and adult patients with tuberous sclerosis. AJR Am J Roentgenol 2004;182:1027-30.

89. Bender BL, Yunis EJ. The pathology of tuberous sclerosis. Pathol Annu 1982;17:339-82.

90. Maziak DE, Kesten S, Rappaport DC, Maurer J. Extrathoracic angiomyolipomas in lymphangioleiomyomatosis. Eur Respir J 1996;9:402-5.

91. Devroede G, Lemieux B, Masse S, Lamarche J, Herman PS. Colonic hamartomas in tuberous sclerosis. Gastroenterology 1988;94:182-8.

92. Gould SR. Hamartomatous rectal polyps are common in tuberous sclerosis. Ann N Y Acad Sci 1991;615:71-80.

93. Martignoni G, Pea M, Reghellin D, Zamboni G, Bonetti F. PEComas: The past, the present and the future. Virchows Arch 2008;452:119-32.